Proceedings of the ASME 2023 International Technical Conference and Exhibition on Packaging and Integration of Electronic and Photonic Microsystems
InterPACK2023
October 24-26, 2023, San Diego, California

IPACK2023-112005

A NUMERICAL STUDY ON THE INFLUENCE OF MIXED CONVECTION HEAT TRANSFER IN SINGLE-PHASE IMMERSION COOLING

Satyam Saini
The University of Texas at Arlington
Arlington, TX

Gautam Gupta
The University of Texas at Arlington
Arlington, TX

Pratik Bansode
The University of Texas at Arlington
Arlington, TX

Pardeep Shahi
The University of Texas at Arlington
Arlington, TX

Vibin Shalom Simon
The University of Texas at Arlington
Arlington, TX

Himanshu Modi
The University of Texas at Arlington
Arlington, TX

Dereje Agonafer
The University of Texas at Arlington
Arlington, TX

Jimil Shah
Stealth Startup
Plano, TX

ABSTRACT

Data centers are critical to the functioning of modern society as they host digital infrastructure. However, data centers can consume significant amounts of energy, and a substantial amount of this energy goes to cooling systems. Efficient thermal management of information technology equipment is therefore essential and allows the user to obtain peak performance from a system and enables higher equipment reliability. Thermal management of data center electronics is becoming more challenging due to rising power densities at the chip level. Cooling technologies like single-phase immersion cooling allow overcoming many such challenges owing to their higher thermal mass, lower fluid pumping powers, and potential component reliability enhancements. It is known that immersion cooling deployments require extremely low coolant flow rates, and, in many cases, natural convection can also be used to sufficiently dissipate the heat from the hot server components. It, therefore, becomes difficult to ascertain whether the rate of heat transfer is being dominated by forced or natural convection. This may lead to ambiguity in choosing an optimal heat sink solution and a suitable system mechanical design due to unknown flow regimes, further leading to sub-optimal system performance. Mixed convection can be used to enhance heat transfer in immersion cooling systems. The present investigation quantifies the contribution of mixed convection using numerical methods in an immersion-cooled server.

An open compute server with dual CPU sockets is modeled on Ansys Icepak with varying power loads of 115W, 160W and 200W. The chosen dielectric fluid for this single-phase immersion-cooled setup is EC-100. Steady-state Computational Fluid Dynamics (CFD) simulations are conducted for forced, natural, and mixed convection heat transfer in a thermally shadowed server configuration at varying inlet flow rates. A baseline heat sink and an optimized heat sink with an increased fin thickness and reduced fin count are utilized for performance comparison. The effect of varying Reynolds number and Richardson number on the heat transfer rate from the heat sink is discussed to assess the flow regime, stability of the flow around the submerged components which depends on the geometry, orientation, fluid properties, flow rate and direction of the flow. The dimensionless numbers' influence on heat transfer rate from a conventional air-cooled heat sink in immersion versus an immersion-optimized heat sink is also compared. The impact of server orientation on heat transfer behavior for the immersion optimized heat sink is also studied on heat transfer behavior for the immersion optimized heat sink.

Keywords: Data Center, Thermal Management, Immersion Cooling, Mixed Convection, Heat Sink

NOMENCLATURE

k	alpha
b	Channel width
t	Fin Thickness

H	Channel Height
Re	Reynolds Number
Nu_b	Average Nusselt Number
Nu_i	Ideal Nusselt Number
Ri	Richardson Number
Ra	Rayleigh Number
SPI	Single-Phase Immersion
CFD	Computational Fluid Dynamic
GWP	Global Warming Potential
PUE	Power Usage Effectiveness

1. INTRODUCTION

Thermal management of data center electronics has become increasingly difficult over the last decade owing to an increase in the utilization of data-intensive technologies such as machine learning, the Internet of things, and cryptocurrency mining. Traditional data center cooling methods that utilize air for heat dissipation of server platforms consume significantly large energy and also water [1]. Liquid-based cooling technologies offer higher heat transfer coefficients and are being increasingly used to dissipate high power densities of the new generation central processing units (CPUs) and graphics processing (GPUs) [2]. Some of the popular liquid cooling technologies include cold plate-based single and two-phase cooling and direct contact single and two-phase immersion cooling. Additional benefits in these cooling technologies have also been proposed using optimized geometrical shape cold plates [3], and the addition of nano-particles to base fluids to improve thermal properties of the base fluids specific to server platform cooling [4,5]. Cooling optimization has also been proposed by using real-time coolant transport modulation techniques either by flow control devices [6,7], chassis modifications [8], or using machine learning algorithms [9] at the server and data center level.

Advanced liquid cooling techniques such as single-phase immersion cooling allow data centers to not only dissipate high power densities but also enable high energy efficiency by offering very low PUE values [10,30]. The primary advantage of single-phase immersion (SPI) cooling lies in the fact that it allows complete removal of fan-based cooling from the servers and any of the synthetic dielectric fluids used are biodegradable with zero global warming potential (GWP) [11,31]. Also, in recent times significant attention has been given to addressing the material compatibility and reliability issues in this cooling technique that had been a major bottleneck in its widespread adoption [12-14]. With the reliability concerns being addressed, the data center industry is now seeing an increase in SPI cooling deployments, especially due to its ease of deployment even in harsh environments where air and hybrid cooling systems cannot be used [12,26].

Coolant flow rates in typical SPI cooled servers usually fall under the laminar flow regime [10,15]. This means if the server is designed with an air-cooled heat sink, it needs to be optimized for lower flow rates and changes in convective heat transfer properties. It also means that under such low Reynolds number flow, it should be carefully analyzed whether the dominant heat transfer mode is forced or natural convection or a combination of both these modes known as mixed convection. Mixed convection is commonly found in cooling systems where the coolant flow rates or flow velocities are very low. In such flows, buoyancy forces have a significant impact on flow behavior and heat transfer rate [16]. Mixed convection is characterized by a dimensionless number known as the Richardson number (Ri) defined by the ratio Gr/Re^2 which is a quantitative indicator of the balance between natural and forced convection in a flow. A value of Ri<1 depicts forced convection-dominated flow and a value of Ri>1 depicts natural convection-dominated flow.

An in-depth review of various convective heat transfer cooling options for electronic packages has been carried out by Incropera [17]. Papanicolaou and Jaluria [18] studied mixed convection in a horizontally oriented square enclosure for a single heat source. They varied the location of the outlet and size of the isothermal heat source assuming laminar 2-D flow with a Re range between 50-2000. It was observed that for Ri values between 0-10, the flow remained in the laminar regime and became oscillatory at higher values. Acharya and Ptankar [19] investigated the effect of buoyancy on laminar mixed convection for a fin-array placed in an enclosure using analytical methods. They observed that heat transfer is significantly affected by the buoyancy forces in laminar mixed convection for such an arrangement of a finned array. Also, an enhancement in heat transfer rate is obtained due to buoyancy-driven secondary flows. Maughan and Incropera [20] experimentally investigated the effects of laminar mixed convection airflow on longitudinal fins between parallel plates where the bottom plate is isothermally heated and the top plate is isothermally cooled. A considerable enhancement in heat transfer was observed for low values of the Rayleigh number (Ra). It was also observed that closely spaced fins had a higher heat transfer rate due to enhanced surface area but this delayed the formation of secondary flows that also enhance heat transfer. Dogan and Sivrioglu [21,22] studied the influence of fin spacing, fin height, and heat flux on laminar mixed convection for longitudinal fins in a rectangular channel. Conclusions were made on optimum fin spacing that yields maximum heat transfer and it was concluded that optimum fin spacing depends on the value of modified Ra.

While there are a lot of studies that look into the impact of forced, natural, or mixed convection separately for finned-arrays in angular ducts and enclosures, there is no discussion about the influence of mixed convection in servers using SPI cooling. Characterization of mixed convection is significant for SPI as a server typically contains multiple heat-dissipating components that may also have an impact on convective heat transfer from the heat sinks. The present investigation aims at characterizing the influence of mixed convection heat transfer in a single server for SPI cooling. A commercially available computational fluid dynamics (CFD) tool, ANSYS Icepak [22], was used to develop the server model and carry out the conjugate heat transfer simulations. The baseline version of the server design is a 2U open rack unit air-cooled chassis design with an air-cooled heat sink. The server was subjected to varying inlet flow rate boundary conditions from fully natural convection to highly forced flow (0<Re<2000). The analysis of mixed convection flow was done by identifying important dimensionless parameters such as Nusselt number, Richardson number, and Rayleigh number. The variation in the influence of mixed convection was observed by varying the geometry of the heat sink to make it more optimized for low flow rate viscous flows. The orientation of the server was also varied from vertical (same direction of flow and natural convection) to horizontal (transverse flow and natural convection directions) to quantify the variation in mixed convection heat transfer. For a constant heat source area (representing the CPU), the source power was also varied at three values of 115W, 160W and 200 W where 115W is the thermal design power of the current CPU design in the server.

2. NUMERICAL MODEL AND ANALYTICAL RELATIONS

This section describes the details of the numerical modeling, its boundary conditions, and the required mathematical background on mixed convection.

2.1 Numerical Modeling and Methodology

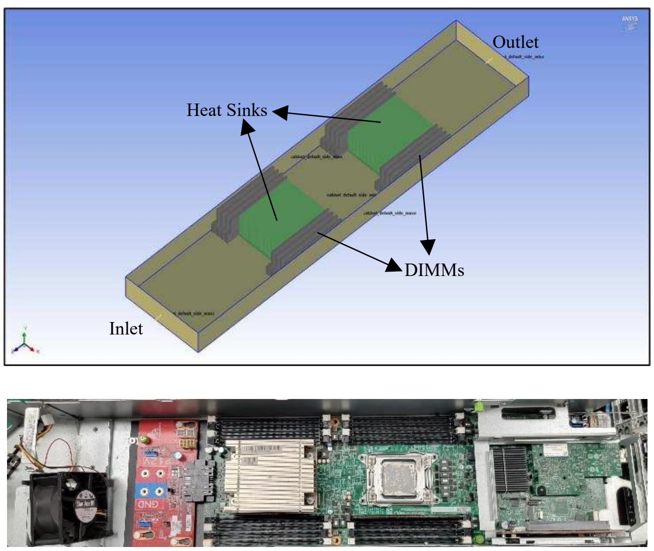

FIGURE 1: OVERVIEW OF THE CFD MODEL SHOWING THE SERVER COMPONENTS AND BOUNDARY CONDITIONS

Figure 1 shows the overview of the numerical model and physical layout of the server used in this study. The server is a 3rd generation Intel-based 3rd generation open compute server with dual CPU sockets, each with maximum thermal design power (TDP) of 115W, in a thermally shadowed configuration [23]. The simplified numerical model of the server was developed with only the CPU as a 2-D heat source under the heat sink base accompanied by the memory modules with no heat dissipation given to the memory modules. Thermo-physical properties of pure aluminum are imparted to the heat sink which was also modeled without the cutouts and the embedded heat pipe. The heat transfer fluid used for the CFD modeling is a synthetic dielectric fluid EC-100. Table 1 shows the overview of the known temperature-dependent properties of the fluid used for the simulation study. A constant value of density for the inlet temperature of 30°C is used during the study due to the limitation of the CFD tool. The thermal performance of this server in SPI with the baseline air-cooled heat sink was experimentally characterized by McWilliams with mineral oil [24]. The results of this experimental study were used to benchmark the baseline CFD model.

TABLE 1: VARIATION OF THERMO-PHYSICAL PROPERTIES OF EC-100 AT DIFFERENT FLUID TEMPERATURES

Temperature	Kinematic Viscosity	Density	Thermal Conductivity	Specific Heat
°C	m^2/s ($\times 10^{-6}$)	kg/m^3	W/mK	J/kgK
30	17.14	839.3	0.138	~2100
40	11.99	832.6	0.130	2209
50	9.52	825.3	0.136	-
60	6.68	819.5	0.135	-
70	5.24	812.9	0.135	-
80	4.22	806.3	0.134	-
90	3.48	799.7	0.133	-
100	2.92	739.1	0.132	2436

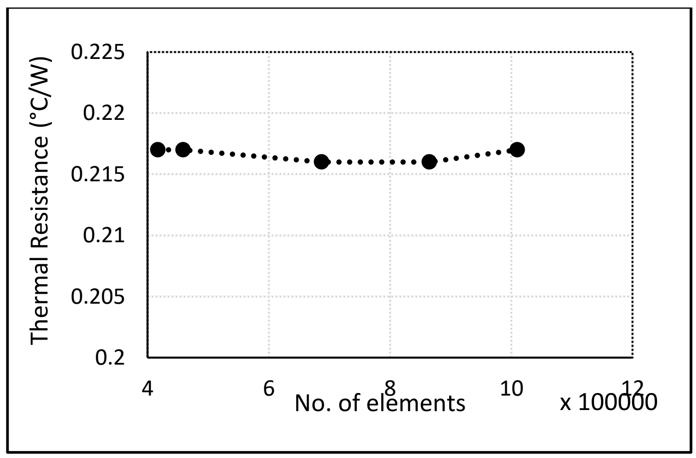

FIGURE 2: RESULTS OF GRID INDEPENDENCE STUDY SHOWING THE VARIATION IN THERMAL RESISTANCE VALUE WITH NUMBER OF MESH ELEMENTS

A grid independence study was first carried out for the baseline CFD model developed as shown in Figure 2. The value of thermal resistance of the heat sink was used to ascertain the grid independence results. The thermal resistance value was observed to be independent of the global mesh size outside of the heat sink and the base value of mesh elements was used for the simulations. For benchmarking the CFD model, the source temperature value was compared with the junction temperature of the server for different inlet flow rates. As can be seen in Figure 3, a close agreement is observed between the experimental data and the CFD modeling results. The maximum difference between the experimental data and the numerical model was observed to be less than 3% for all the simulation cases. The slight variation could be attributed to different fluids being used in both the experimental and numerical study (mineral oil for experimental and thermally enhanced synthetic fluid for CFD). The thermal performance was also reduced in the CFD modeling as the no heat pipes were modeled.

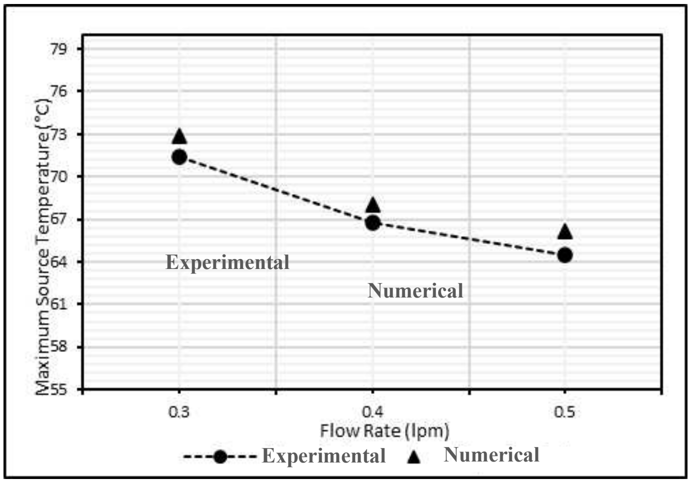

FIGURE 3: COMPARISON OF THE EXPERIMENTAL RESULTS AND RESULTS FROM THE NUMERICAL MODELED

To vary the Re values, the inlet flow rate was varied by defining a velocity inlet boundary condition. The source power is varied for three values of 115 W, 160 W and 200 W. To quantify the participation of mixed convection for low flow rate viscous flows where natural convection may be assumed to be the dominating heat transfer mode, the baseline air-cooled heat sink design was assumed to be not beneficial. A few studies in the current literature also point to this fact [25, 27]. As these studies conclude, immersion optimized parallel plate-fin heat sinks result in thicker fins with reduced fin count [28]. Taking this as the base assumption, two different fin count and fin thickness heat sinks were modeled, a baseline heat sink and an optimized heat sink with an increased fin thickness and reduced fin count. The fincount for the baseline heatsink is taken as 35 and the fin thickness is 0.23 mm. On the other hand, the fin count for the optimized heatsink is taken as 25 and the fin thickness is 0.59mm. The heatsink height remained the same as 41 mm in both the cases.

2.2 Analytical Relations and Governing Equations

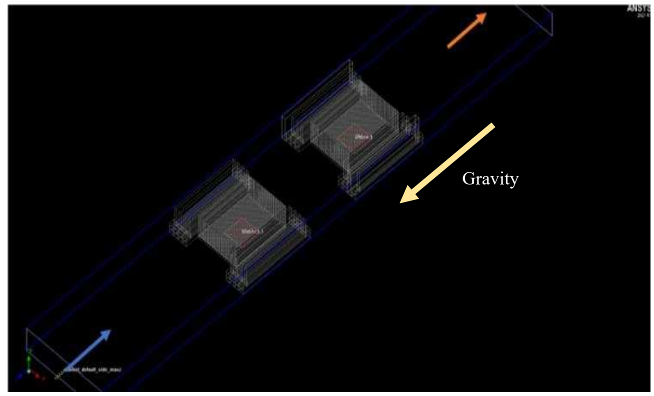

FIGURE 4: OVERVIEW OF THE BOUNDARY CONDITIONS USED FLOW DIRECTION AND DIRECTION OF THE GRAVITY

ANSYS Icepak [22] solves Navier-Stokes equations of mass, momentum, species, and energy to calculate heat transfer in laminar flow conditions. Additional transport equations of turbulence and radiation can be used if the flow and heat transfer involves these phenomena, which was not the case for the current study. These equations are written as follows:

Mass conservation:

$$\frac{\partial \rho}{\partial t} + \nabla.(\rho\vec{v}) = 0 \qquad (1)$$

The above equation reduces to $\nabla.(\vec{v}) = 0$ for incompressible fluids.

Momentum equation:

$$\frac{\partial}{\partial t}(\rho\vec{v}) + \nabla.(\rho\vec{v}\vec{v}) = -\nabla p + \nabla.(\bar{\bar{\tau}}) + \rho\vec{g} + \vec{F} \qquad (2)$$

Energy Equation:

$$\frac{\partial}{\partial t}(\rho h) + \nabla.(\rho h\vec{v}) = \nabla.[(k + k_t)\nabla T] + S_h \qquad (3)$$

Here, the fluid energy equation is written in terms of sensible enthalpy, h. k is the molecular conductivity and k_t is the turbulence transport conductivity. The source term S_h represents user-defined volumetric heat sources. For the solid regions, the energy equation due to conduction within the solid looks as follows:

$$\frac{\partial}{\partial t}(\rho h) = \nabla.(k\nabla T) + S_h \qquad (4)$$

Here, k is the thermal conductivity of the solid, ρ is the density, T is the temperature and S_h is the source term for volumetric heat sources.

For buoyancy-driven flows in mixed or fully natural convection-driven flows are simulated using the Bousinessq model for natural convection. This model treats density as constant in all solved equations except the buoyancy term in the momentum equation:

$$(\rho - \rho_0)g \approx -\rho_0 \beta (T - T_0) g \qquad (5)$$

In the above equation, ρ_0 is the constant density of the fluid, T_0 is the operating temperature and β is the volume expansion coefficient of the fluid.

The impact of various inlet boundary conditions on the heat transfer behavior using the baseline air-cooled heat sink as compared to an immersion optimized heat sink was calculated using an analytical model for parallel plate heat sinks [29]. This model predicts the average heat transfer rate using a composite solution for fully developed and developing flows in a single channel of an 'n' channel parallel plate heat sink. The model assumes that the fins are isothermal and have the temperature of the base, assuming the material has a high thermal conductivity. The model also includes the effect of fin efficiency and combines the impact of ideal heat transfer rate (Nu_i) and average heat transfer rate (Nu_b). The model uses a modified Reynolds number value which is a dimensionless number combining the basic definition of the Reynolds number with dimensionless channel width as,

$$Re_b^* = Re_b . \frac{b}{L} \qquad (6)$$

Here, L is the channel length and b is the channel width. Re_b is a dimensionless Reynolds number calculate using channel width as the characteristic length. The average heat transfer coefficient is related to the ideal value of the Nusselt number (for a fin with η=1) by,

$$h = Nu_i . \frac{k_f}{b} \qquad (7)$$

where k_f is the fluid conductivity. The final composite model is defined as in equation 8,

$$Nu_b = \frac{tanh\sqrt{2Nu_i \frac{k_f}{k}\frac{H}{b}\frac{H}{t}\left(\frac{t}{L}+1\right)}}{\sqrt{2Nu_i \frac{k_f}{k}\frac{H}{b}\frac{H}{t}\left(\frac{t}{L}+1\right)}} * Nu_i \qquad (8)$$

Where Nu_i

$$Nu_i = \{[\frac{Re_b^* Pr}{2}]^{-3} + ((0.664\sqrt{Re_b^*}Pr^{1/3}) X \left(\sqrt{1+\frac{3.65}{\sqrt{Re_b^*}}}\right)^{-3}\}^{-1/3} \qquad (9)$$

Here k is the thermal conductivity of the solid, t is the fin thickness and H is fin height.

Also, Richardson Number (Ri) is defined as the ratio of the buoyancy-induced flow to the forced flow within a fluid system. It helps assess the relative significance of natural convection (caused by buoyancy forces) compared to forced convection (caused by external means such as fans or pumps).

The Richardson Number is expressed as:

$$Ri = \frac{(g\ \beta\ \Delta T\ L^3)}{(\nu^2 U)} \qquad (10)$$

where, g is the acceleration due to gravity, β is the coefficient of thermal expansion, ΔT is the temperature difference across the fluid, L is a characteristic length or height scale, ν is the kinematic viscosity of the fluid, and U is the characteristic velocity of the fluid flow.

3. RESULTS AND DISCUSSION

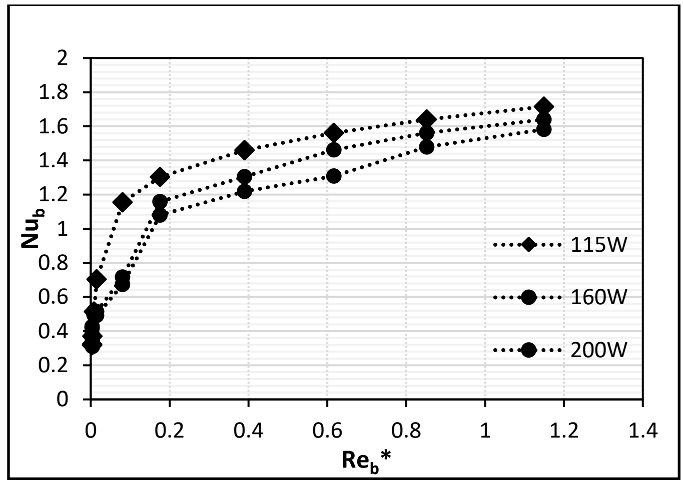

FIGURE 5: HEAT TRANSFER BEHAVIOR OF THE BASELINE AIR-COOLED HEAT SINK AT 115W, 160W AND 200W FOR VARIOUS MODIFIED REYNOLDS NUMBER VALUES

It was also observed that the heat transfer behavior saturates after a certain flow rate or Reynolds number value. This Reynolds number value occurs at a very high flow rate which will be redundant for the current server's total heat dissipation value. It should also be noted that an optimized heat sink for 160W and 200 W may give a better thermal performance as opposed to the current trend. Figure 5 shows the heat transfer behavior for the baseline heat sink at 115W, 160 W and 200W. It is seen that the value of the modified Nusselt number reduces to almost half of the value in the immersion optimized heat sink case implying that the heat transfer behavior is significantly impacted if an unoptimized heat sink is used, especially for low flow rate values.

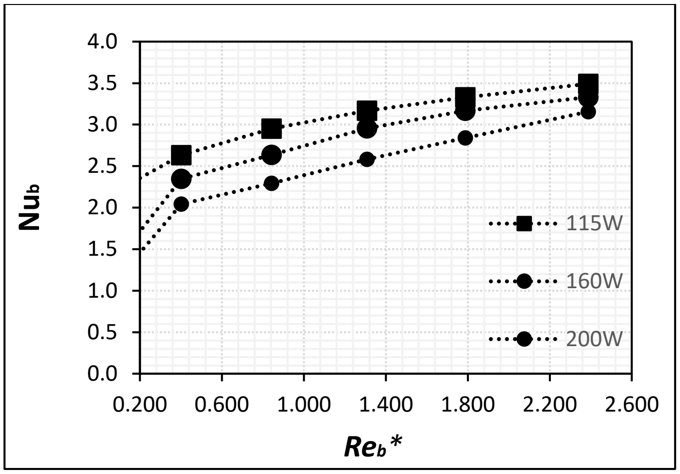

FIGURE 6: MODIFIED NUSSELT NUMBER VS MODIFIED REYNOLDS NUMBERS FOR THE OPTIMIZED HEAT SINK

Figure 6 shows the variation of the modified Nusselt number with varying modified Reynolds numbers for the immersion optimized heat sink when the server is immersed vertically. The modified Nusselt and Reynolds numbers are calculated using the channel width as the hydraulic diameter instead of the wetted channel cross-section and perimeter. It was observed that the heat transfer behavior at low Reynolds number values is initially better for the 160 W and 200 W CPU power for the same heat sink than 115 W CPU power as seen in Table 2. This could be because, at very low flow rates, higher CPU power induces a greater amount of natural convection behavior that assists in better heat transfer. After that, as the heat sink has been optimized for a power value of 115 W, the heat sink produces better heat transfer for that power value thereon.

TABLE 2: COMPARISION OF THE HEAT TRANSFER RATE FOR 115 W, 160 W, AND 200 W OF CPU POWER FOR VARYING MODIFIED REYNOLDS NUMBER

115 W		160 W		200W	
Re_b*	Nu_b	Re_b*	Nu_b	Re_b*	Nu_b
0.007	0.66	0.007	0.727	0.007	0.794
0.007	0.65	0.007	0.744	0.007	0.801
0.009	0.76	0.009	0.727	0.009	0.793
0.020	1.29	0.020	0.804	0.020	0.861
0.037	1.66	0.037	1.335	0.037	1.176
0.190	2.34	0.190	1.684	0.190	1.431
0.401	2.63	0.401	2.347	0.401	2.043
0.843	2.95	0.843	2.634	0.843	2.295
1.307	3.17	1.307	2.955	1.307	2.583
1.788	3.33	1.788	3.167	1.788	2.841
2.388	3.49	2.388	3.331	2.388	3.156

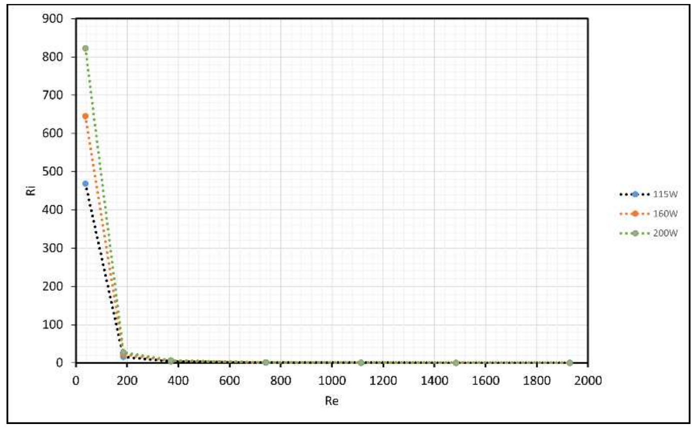

FIGURE 7: RICHARDSON NUMBER VS REYNOLDS NUMBER FOR THE OPTIMIZED HEAT SINK

Figure 7 shows the variation of the mixed convection behavior for the optimized heat sink at 115 W, 160 W, and 200 W CPU power. Mixed convection behavior is quantified by calculating the value of the Richardson number which is the ratio of the Grashof number to the square of the Reynolds number value. A value of Ri=1 depicts that both force and natural convection are balanced. A value of Ri<1 indicates that the heat transfer is dominated by forced convection and a value of Ri>1 indicates natural convection-dominated flow. It was observed that the heat transfer inside the given server is dominated by natural convection until a Reynolds number value of approximately 730 for both the power values investigated. This value of the Reynolds number depicts a very large flow rate which for this heat server will be redundant. Thus it can be assumed that the heat transfer behavior in this server is dominated by natural convection.

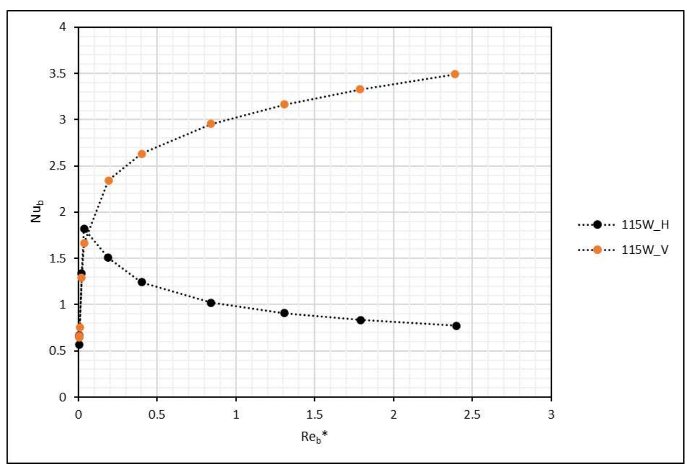

FIGURE 8: INFLUENCE OF SERVER ORIENTATION ON THE MODIFIED NUSSELT NUMBER AND MODIFIED REYNOLDS NUMBERS AT 115 W

Figure 8 shows the influence of server orientation on heat transfer behavior for the immersion optimized heat sink for 115W CPU power based off the CFD simulations. It can be seen that for the optimized heat sink in the vertical orientation, the heat transfer rate keeps increasing even though it appears to be saturating for high flow rate values. When the server is kept in horizontal orientation, depicting that the forced flow direction is orthogonal to the direction of the gravity vector. For the horizontal immersion case, the heat transfer behavior saturates after increasing rapidly and then starts reducing as the flow rate is increased further. This means, that for horizontal orientation if the impact of natural convection is reduced, the overall heat transfer will reduce after a certain flow rate. This flow rate must be quantified for the servers if a horizontal immersion case so that the thermal performance of the server is not compromised in operational conditions.

4. CONCLUSION

This study numerically investigated the influence of mixed convection heat transfer in a single server SPI cooling. With increasing, edge deployments and expansion of 5G, natural convection-based immersion tanks operating at elevated ambient temperatures will be useful owing to simple cooling infrastructure and high heat capture capabilities. The following conclusions were drawn from this investigation:

- For the current server design and power values analyzed, natural convection is concluded to be the dominant heat transfer mode
- Mixed convection conditions are observed at very high liquid flow rate conditions that are operationally not feasible in single-phase immersion cooling
- Immersion optimized heat sink performs better in both vertical and horizontal server orientations
- Immersion optimized heat sink also outperformed baseline heat sink outside the optimized power range
- The point at which natural and forced convection are balanced occurs at a very large flow rate value for the current server
- For server horizontally immersed server, the peak heat transfer point should be characterized as a sharp decrease in heat transfer that occurs thereafter

5. REFERENCES

[1] Li, Z., & Satish G. Kandlikar, S.G., 2015, "Current Status and Future Trends in Data-Center Cooling Technologies," Heat Transfer Engineering, 36(6), 523-538, DOI: 10.1080/01457632.2014.939032

[2] ASHRAE, 2021, "Emergence and expansion of liquid cooling, American Society of Heating, Refrigeration and Air-Conditioning Engineers," Atlanta, GA

[3] Hoang, C.H., Rangarajan, S., Khalili, S., Ramakrisnan, B., Radmard, V., Hadad, Y., Schiffres, S., Sammakia, B., 2021, "Hybrid microchannel/multi-jet two-phase heat sink: A benchmark and geometry optimization study of commercial product," International Journal of Heat and Mass Transfer, Volume 169, 120920, ISSN 0017-9310, https://doi.org/10.1016/j.ijheatmasstransfer.2021.120920.

[4] Shahi, P., Agarwal, S., Saini, S., Niazmand, A., Bansode, P., & Agonafer, D., 2020, "CFD Analysis on Liquid Cooled Cold Plate Using Copper Nanoparticles." *Proceedings of the ASME 2020 International Technical Conference and Exhibition on Packaging and Integration of Electronic and Photonic Microsystems*. *ASME 2020 International Technical Conference and Exhibition on Packaging and Integration of Electronic and Photonic Microsystems*. Virtual, Online. October 27–29, V001T08A007. ASME. https://doi.org/10.1115/IPACK2020-2592

[5] Niazmand, A., Murthy, P., Saini, S., Shahi, P., Bansode, P., & Agonafer, D., 2020, "Numerical Analysis of Oil Immersion Cooling of a Server Using Mineral Oil and Al2O3 Nanofluid." *Proceedings of the ASME 2020 International Technical Conference and Exhibition on Packaging and Integration of Electronic and Photonic Microsystems*. *ASME 2020 International Technical Conference and Exhibition on Packaging and Integration of Electronic and Photonic Microsystems*. Virtual, Online. October 27–29, V001T08A009. ASME. https://doi.org/10.1115/IPACK2020-2662

[6] P. Shahi, S. Saini, P. Bansode and D. Agonafer, "A Comparative Study of Energy Savings in a Liquid-Cooled Server by Dynamic Control of Coolant Flow Rate at Server Level," in IEEE Transactions on Components, Packaging and Manufacturing Technology, vol. 11, no. 4, pp. 616-624, April 2021, doi: 10.1109/TCPMT.2021.3067045.

[7] Shahi, P., Deshmukh, A. P., Hurnekar, H. Y., Saini, S., Bansode, P., Kasukurthy, R., and Agonafer, D., 2022 "Design, Development, and Characterization of a Flow Control Device for Dynamic Cooling of Liquid-Cooled Servers," ASME. *J. Electron. Packag*., 144(4): 041008. https://doi.org/10.1115/1.4052324

[8] Modi, H., 2020, "Computational Study of Air-Cooled Servers with Improved Ducting and Chassis Re-Design," M.S Thesis, The University of Texas at Arlington, Arlington, TX.

[9] Kumar, R., Khatri, S.K., and Diván, M.J., 2021, "Data Center Air Handling Unit Fan Speed Optimization Using Machine Learning Techniques," *9th International Conference on Reliability, Infocom Technologies and Optimization (Trends and Future Directions) (ICRITO)*, pp. 1-10, doi: 10.1109/ICRITO51393.2021.9596311.

[10] Eiland, R., Fernandes, J., Vallejo, M., Agonafer, D., and Mulay, V., 2014, "Flow Rate and inlet temperature considerations for direct immersion of a single server in mineral oil," *Fourteenth Intersociety Conference on Thermal and Thermomechanical Phenomena in Electronic Systems (ITherm)*, May 27-30, Orlando, FL, pp. 706-714, doi: 10.1109/ITHERM.2014.6892350.

[11] Murthy, Prajwal, Gautam Gupta, Joseph Herring, Jacob Lamotte-Dawaghreh, Krishna Bhavana Sivaraju, Pratik Bansode, Himanshu Modi, Dereje Agonafer, Poornima Mynampati, and Mike Sweeney. "*CFD Simulation-Based Comparative Study of Forced Convection Single-Phase Liquid Immersion Cooling for a High-Powered Server.*" In International Electronic Packaging Technical Conference and Exhibition, vol. 86557, p. V001T01A006. American Society of Mechanical Engineers, 2022.

[12] Shah, J. M., Padmanaban, K., Singh, H., Duraisamy Asokan, S., Saini, S., and Agonafer, D., 2021, "Evaluating the Reliability of Passive Server Components for Single-Phase Immersion Cooling." ASME. *J. Electron. Packag*., 144(2): 021109. https://doi.org/10.1115/1.4052536

[13] Bansode, Pratik V., Jimil M. Shah, Gautam Gupta, Dereje Agonafer, Harsh Patel, David Roe, and Rick Tufty. "Measurement of the thermal performance of a custom-build single-phase immersion cooled server at various high and low temperatures for prolonged time." *Journal of Electronic Packaging* 142, no. 1 (2020): 011010.

[14] Open Compute Project, 2022, "Immersion Requirements Revision 2.0," Available at: https://www.opencompute.org/documents/ocp-acs-immersion-requirements-rev-2-v1-00-pdf

[15] Cheng, C.C., Chang, P.C., Li, H.C., Hsu, F.I., 2020, "Design of a single-phase immersion cooling system through experimental and numerical analysis," International Journal of Heat and Mass Transfer, 160, 120203, ISSN 0017-9310, https://doi.org/10.1016/j.ijheatmasstransfer.2020.120203

[16] S.G. Taji, G.V. Parishwad, N.K. Sane, Enhanced performance of horizontal rectangular fin array heat sink using assisting mode of mixed convection, International Journal of Heat and Mass Transfer, Volume 72, 2014, Pages 250-259, ISSN 0017-9310, https://doi.org/10.1016/j.ijheatmasstransfer.2014.01.012

[17] Incropera, F. P. (November 1, 1988). "Convection Heat Transfer in Electronic Equipment Cooling." ASME. J. Heat Transfer. November 1988; 110(4b): 1097–1111. https://doi.org/10.1115/1.3250613

[18] Papanicolaou, E., and Jaluria, Y., 1991, "Mixed Convection From an Isolated Heat Source in a Rectangular Enclosure," Numer. Heat Transfer, Part A, 18(4), pp. 427-461, DOI: 10.1080/10407789008944802

[19] Acharya, S., and Patankar, S. V., 1981, "Laminar Mixed Convection in a Shrouded Fin Array," ASME. J. Heat Transfer, 103(3): 559–565. https://doi.org/10.1115/1.3244502

[20] Maughan, J. R., and Incropera, F. P., 1990, "Mixed Convection Heat Transfer With Longitudinal Fins in a Horizontal Parallel Plate Channel: Part II—Experimental Results," ASME. *J. Heat Transfer*, 112(3): 619–624. https://doi.org/10.1115/1.2910432

[21] Dogan, M. and Sivrioglu, M., 2010, "Experimental investigation of mixed convection heat transfer from longitudinal fins in a horizontal rectangular channel," *International Journal of Heat and Mass Transfer*, *53*(9-10), pp.2149-2158, https://doi.org/10.1016/j.ijheatmasstransfer.2009.12.031

[22] Ansys® Icepak, Release 2021R1, ANSYS, Inc.

[23] Ning, J., "Intel server in open Rack Hardware v 0.3," https://www.yumpu.com/en/document/read/29317108/intel-server-in-open-rack-hardware-v03-open-compute-project

[24] McWilliams, T.D., 2014, "Evaluating Heat Sink Performance In An Immersion-cooled Server System," M.S Thesis, The University of Texas at Arlington, Arlington, TX

[25] Shah, J.M., Dandamudi, R., Bhatt, C., Rachamreddy, P., Bansode, P., & Agonafer, D., 2019, "CFD Analysis of Thermal Shadowing and Optimization of Heatsinks in 3rd Generation Open Compute Server for Single-Phase Immersion Cooling," *Proceedings of the ASME 2019 International Technical Conference and Exhibition on Packaging and Integration of Electronic and Photonic Microsystems*. *ASME 2019 International Technical Conference and Exhibition on Packaging and Integration of Electronic and Photonic Microsystems*. Anaheim, California, USA. October 7–9, 2019. V001T02A015. ASME. https://doi.org/10.1115/IPACK2019-6600

[26] Sivaraju, Krishna Bhavana, Pratik Bansode, Gautam Gupta, Jacob Lamotte-Dawaghreh, Satyam Saini, Vibin Simon, Joseph Herring, Saket Karajgikar, Veerendra Mulay, and Dereje Agonafer. "Comparative Study of Single-Phase Immersion Cooled Two Socket Server in Tank and Sled Configurations." In *International Electronic Packaging Technical Conference and Exhibition*, vol. 86557, p. V001T01A010. American Society of Mechanical Engineers, 2022.

[27] Sarangi, S., McAfee, E.D., Damm, D.G., and Gullbrand, J., 2022, "Single-Phase Immersion Cooling Performance in Intel Servers with Immersion Influenced Heatsink Design," *38th Semiconductor Thermal Measurement, Modeling & Management Symposium (SEMI-THERM)*, 21-25 March, San Jose, CA, pp. 1-5.

[28] Saini, Satyam, Tushar Wagh, Pratik Bansode, Pardeep Shahi, Joseph Herring, Jacob Lamotte-Dawaghreh, Jimil M. Shah, and Dereje Agonafer. "A Numerical Study on Multi-Objective Design Optimization of Heat Sinks for Forced and

Natural Convection Cooling of Immersion-Cooled Servers." Journal of Enhanced Heat Transfer 29, no. 8 (2022).

[29] Teertstra, P., Yovanovich, M.M. and Culham, J.R., 2000, "Analytical forced convection modeling of plate fin heat sinks," *Journal of Electronics Manufacturing*, *10*(04), pp.253-261.

[30] Bansode, Pratik V., Jimil M. Shah, Gautam Gupta, Dereje Agonafer, Harsh Patel, David Roe, and Rick Tufty. "Measurement of the thermal performance of a single-phase immersion cooled server at elevated temperatures for prolonged time." In *International Electronic Packaging Technical Conference and Exhibition*, vol. 51920, p. V001T02A010. American Society of Mechanical Engineers, 2018.

[31] Shinde, Pravin A., Pratik V. Bansode, Satyam Saini, Rajesh Kasukurthy, Tushar Chauhan, Jimil M. Shah, and Dereje Agonafer. "Experimental analysis for optimization of thermal performance of a server in single phase immersion cooling." In *International Electronic Packaging Technical Conference and Exhibition*, vol. 59322, p. V001T02A014. American Society of Mechanical Engineers, 2019.

